Probing different nuclear shapes via the decay of giant dipole resonance in hot rotating nuclei

Deepak Pandit*
Variable Energy Cyclotron Centre, 1/AF Bidhan Nagar, Kolkata 700064

Abstract

The giant dipole resonance (GDR) lineshapes have been studied from α-like and non-α-like nuclei in the reactions ^{20}Ne ($E_{\rm lab}$ = 145, 160 MeV) + ^{12}C and ^{20}Ne ($E_{\rm lab}$ = 160 MeV) + ^{27}Al, populating ^{32}S and ^{47}V, respectively. The non-α-like ^{47}V undergoes Jacobi shape transition and matches exceptionally well with the theoretical GDR lineshape estimated under the framework of thermal shape fluctuation model (TSFM). On the other hand, for α-cluster ^{32}S an extended prolate kind of shape is observed which is predicted to be due to the formation of orbiting dinuclear configuration or molecular structure of ^{16}O + ^{16}O in the ^{32}S superdeformed band.

1. Introduction

The giant dipole resonance (GDR), built on highly excited nuclear states, is the main experimental probe to study the shapes of hot rotating nuclei [1]. Hot nuclei are formed in heavy ion fusion reactions where the relative kinetic energy of the colliding nuclei is converted into internal excitation energy and high angular momentum (J) of the compound nuclei. These nuclei at high spin may undergo a Jacobi shape transition, an abrupt change of shape from an oblate ellipsoid rotating around the symmetry axis to an elongated prolate or triaxial shape rotating perpendicularly around the symmetry axis, similar to one, which occurs in rotating gravitating stars [2]. In the search for exotic nuclear shapes, the light and medium mass nuclei are of special interest. This is because these nuclei are expected to undergo Jacobi shape transition at values of the angular momentum which are relatively low and below the fission limit. Meanwhile, the phenomena of clustering and large deformations in light $N = Z$ nuclei has evoked an intense theoretical and experimental efforts to search for highly (super/hyper) deformed (SD/HD) nuclear systems [3, 4]. There are indications that such highly deformed shapes are likely to be observed in light α-like systems ($A_{\rm CN}$ $\sim$ 20-60) at higher angular momenta (typically, $\geq$ 15$\hbar$) and excitation energies (typically, $\geq$ 40 MeV). The aim of the present study is to make quantitative experimental estimation of the deformed shapes of light α and non-α like systems using GDR lineshape studies.

The GDR, a particularly interesting mode of collective vibration, can be understood as out of phase oscillations of the protons and the neutrons in the nucleus [1]. It occurs on a time scale that is sufficiently short ($\sim 10^{22}$ s) and thus provides information prevailing at that time. Interestingly, the resonance energy being inversely proportional to the

*email: deepak.pandit@vecc.gov.in

nuclear radius one gets a single Lorentzian strength function for spherical nuclei since the vibrations along the three principal axes are same. However, the GDR strength function splits in the case of deformed nuclei and the investigation of this strength distribution gives a direct access to look into nuclear deformations [1, 5]. The decay of GDR γ-rays from hot ^{32}S and ^{47}V nuclei have been studied to explore the deformed shapes of light α and non-α like systems at high angular momentum using GDR lineshape and compare them with the corresponding predictions for equilibrium Jacobi shapes.

2. Experimental setup

A suitable detector system is an important part of the high-energy γ-measurement. In order measure the high energy γ-rays from the decay of GDR (5–25 MeV), a Large Area Modular BaF_2 Detector Array (LAMBDA) [6] has been designed, developed and fabricated at the Variable Energy Cyclotron Centre (VECC). The entire detector system has been fabricated from bare BaF_2 crystals with indigenous in-house expertise. The gamma spectrometer consists of 162-individual detector elements in a planar and modular geometry, each having a cross-section of 3.5 cm $\times$ 3.5 cm and a length of 35 cm. The details can be found in Ref[6]. Along with the LAMBDA spectrometer, a 50-element gamma-multiplicity filter made of BaF_2 has also been designed and developed for the measurement of angular momentum of the compound nucleus in an event by event mode [7]. Standard procedures were followed for multiplicity detector fabrication from bare barium fluoride crystals (3.5 cm $\times$ 3.5 cm and a length of 35 cm). First, the bare crystals were cleaned thoroughly using pure dehydrated ethyl alcohol. Each crystal was wrapped with 6 layers of 15 μm white teflon tape since the scintillation light components are in the ultra violet (UV) region and teflon (C_2F_2) is a very good reflector of UV light. Next, aluminium foil of 10 μm (3–4 layers) was used to enhance the light collection and to block the surrounding light from entering into the crystal. Fast, UV sensitive photomultiplier tubes (29 mm diameter, Phillips XP2978) were coupled with the crystals using highly viscous UV transmitting optical grease (Basylone, 300000 cstokes). Specially designed aluminium collars were also used around the coupling area to provide additional support. A squared shape teflon reflector (3.5 cm $\times$ 3.5 cm) with a 3.0 cm hole at the centre was placed at the PMT end of the crystal to reflect back UV light which would otherwise escape from the PMT. A PMT voltage divider base was then attached to the PMT for applying the high voltage. Finally, the whole assembly was covered with black electrical tape for light-tightness and with heat-shrinkable PVC tube for providing mechanical stability to the detector. Next, the individual detector elements were tested with lab standard gamma ray sources. The observed energy resolution was 7.2% at 1.17 MeV of ^{60}Co source while the time resolution obtained was 450 ps. The crosstalk probability was 12% at 662 keV for 200 keV threshold [7]. After fabrication, it was employed in an in-beam experiment along with the LAMBDA spectrometer to study angular momentum gated GDR γ-rays from ^{47}V and ^{32}S.

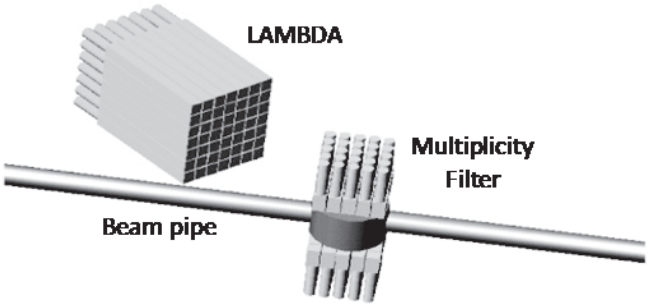

Figure 1: Schematic view of the experimental setup for LAMBDA (Large BaF_2 Array) spectrometer in a 7×7 matrix arrangement along with the low energy γ-ray multiplicity filter.

3. Experimental details and data analysis

The ^{47}V and ^{32}S nuclei were formed by bombarding pure 1 mg/cm^2 thick ^{27}Al and ^{12}C targets, respectively, with accelerated ^{20}Ne beams from the K-130 cyclotron at VECC [8]. The ^{47}V nucleus was populated at an excited energy of 108 MeV corresponding to a projectile energy of 160 MeV. Similarly, the initial excitation energies of ^{32}S nucleus were 73 & 78 MeV corresponding to projectile energies of 145 & 160 MeV. The critical angular momenta for the two systems ^{47}V and ^{32}S were $38\hbar$ and $24\hbar$ respectively and extend well beyond the critical angular momentum values of $29.6\hbar$ and $21.5\hbar$ at which the Jacobi transitions are predicted to occur for these nuclei (according to systematic $J_c = 1.2A^{5/6}$ [9]). The angular momentum values are also well below their fission limits for the two systems making it possible to probe these nuclei at these conditions. The high-energy photons were detected using the LAMBDA detector array [6]. A part of the LAMBDA spectrometer (49 detectors) arranged in a 7×7 matrix was centered at 55° to the beam direction and at a distance of 50 cm from the target. Along with the LAMBDA spectrometer, the 50-element multiplicity filter was employed to measure the γ-multiplicities to extract the angular momentum in coincidence with the high-energy photon events. The multiplicity filter was split into two blocks of 25 detectors each and was placed on the top and the bottom of the scattering chamber at a distance of 10 cm from the target center (covering 30% of 4π) in castle geometry [8]. The schematic view of the experimental setup is shown in Figure 1.

The high-energy gamma spectra were extracted from the off-line analysis of the data recorded in the event-by-event mode by applying proper cuts on the Time-Of-Fight (TOF) and Pulse Shape Discrimination (PSD). After application of different conditions, in a valid event, the energy deposited in the detectors was summed using a nearest neighbor event reconstruction technique [6]. Finally the energies were Doppler corrected assuming the source velocity same as the compound nucleus velocity. The measured fold distributions from the multiplicity filter were mapped onto the angular momentum distributions using a realistic approach based on Monte Carlo GEANT simulation [7]. In this simulation, the realistic experimental conditions (including the detector threshold and trigger condition) were taken into account. Two blocks of 25 detectors arranged in 5×5 arrays were kept on the top and bottom of the scattering chamber, similar to the experiment. The incident multiplicity distribution was considered triangular given as

$$P(M) = \frac{2M+1}{1+\exp\left(\frac{(M-M_{\max})}{\delta_m}\right)} \qquad (1)$$

where, $M_{\max}$ is the maximum of this distribution and δm is the diffuseness. The different input multiplicities of the low energy γ-rays were obtained by creating a random number according to the multiplicity distribution $P(M)$. Low energy gamma rays, for each randomly generated multiplicity, were thrown isotropically from the target centre and the corresponding fold was recorded for that event. The energy distribution of the incident multiplicity was considered a Gaussian with peak at 0.5 MeV and width 0.65 MeV. The angular momentum distribution of the reaction ^{20}Ne+^{27}Al was obtained from statistical model code CASCADE. The conversion of the angular momentum distribution to multiplicity distribution was achieved using the relation $J = 2M+C$, where C is the free parameter which takes into account the angular momentum loss due to particle evaporation and emission of statistical γ-rays. The parameters $M_{\max}$ and δ_m of the multiplicity distribution was obtained from the J-distribution by varying the free parameter C

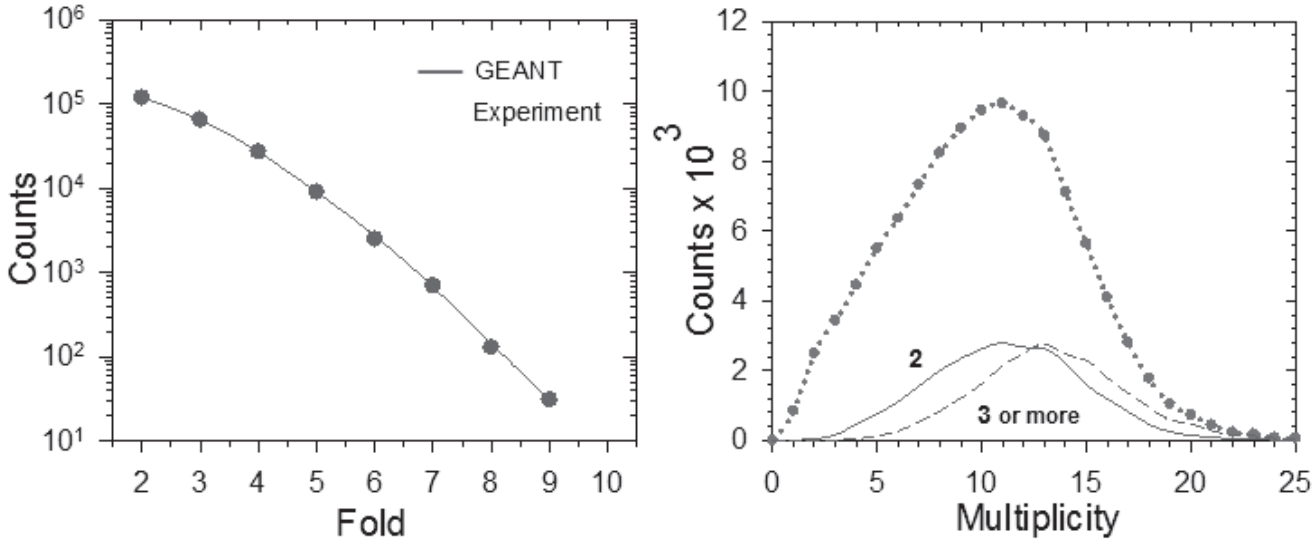

Figure 2: [Left] The experimental fold spectrum fitted with GEANT simulation. [Right] The incident multiplicity distribution used in GEANT simulation (symbols with dotted line) along with the multiplicity distributions obtained for different folds.

until the best fit to the measured F-distribution was achieved. The value of C was obtained as 6 and the parameters of the M-distribution were extracted as $M_{\max} = 14.0$ and $\delta_m = 2$ for best fit. The high-energy γ-ray spectra for ^{47}V were generated for fold 2 and fold ≥ 3 in the multiplicity filter which correspond to average angular momentum values of $28\hbar$ and $31\hbar$, respectively. The experimental fold distribution and the simulated fold distribution generated using GEANT3 are shown in Figure 2 along with the incident multiplicity distribution (dotted line with symbols) and the multiplicity distributions for different fold windows. The high-energy spectra for ^{32}S were generated for folds ≥ 3 for both the energies 145 & 160 MeV. Next, the experimental high-energy γ-ray spectra were fitted using the statistical model decay code CASCADE [10, 11] along with a bremsstrahlung component to extract the GDR strength functions. The estimated spin distributions, using GEANT3 simulation for different folds, were used as inputs in the statistical model calculation. The non statistical contribution arising due to bremsstrahlung was parameterized using the relation $\sigma_{\rm brem} = A \cdot \exp(E_\gamma/E_0)$. The slope parameter was taken according to the prediction $E_0 = 1.1[(E_{\rm lab}V_c)/A_p]^{0.72}$, where $E_{\rm lab}$, V_c and A_p are the beam energy, Coulomb barrier and projectile mass, respectively [12]. The level density prescription of Ignatyuk *et al.*, [13] was used in the CASCADE with the asymptotic level density parameter $\tilde{a} = A/8.0$ MeV^1. Finally, the theoretical spectrum was folded with the detector response function, generated using the Monte Carlo GEANT3 simulation, to compare with the experimental spectrum [6]. The linearized GDR spectra for ^{47}V (for two angular momentum windows) and ^{32}S (for two incident energies) are shown in Figure 3 along with the GDR strength functions used in the CASCADE calculations. The extracted GDR parameters are listed in Table-1 and Table-2 for ^{47}V and ^{32}S, respectively.

4. Results and discussion

It is very interesting to note that the GDR lineshapes for the two systems are completely different from each other. Moreover, the lineshapes also remarkably different from the one usually gets in the

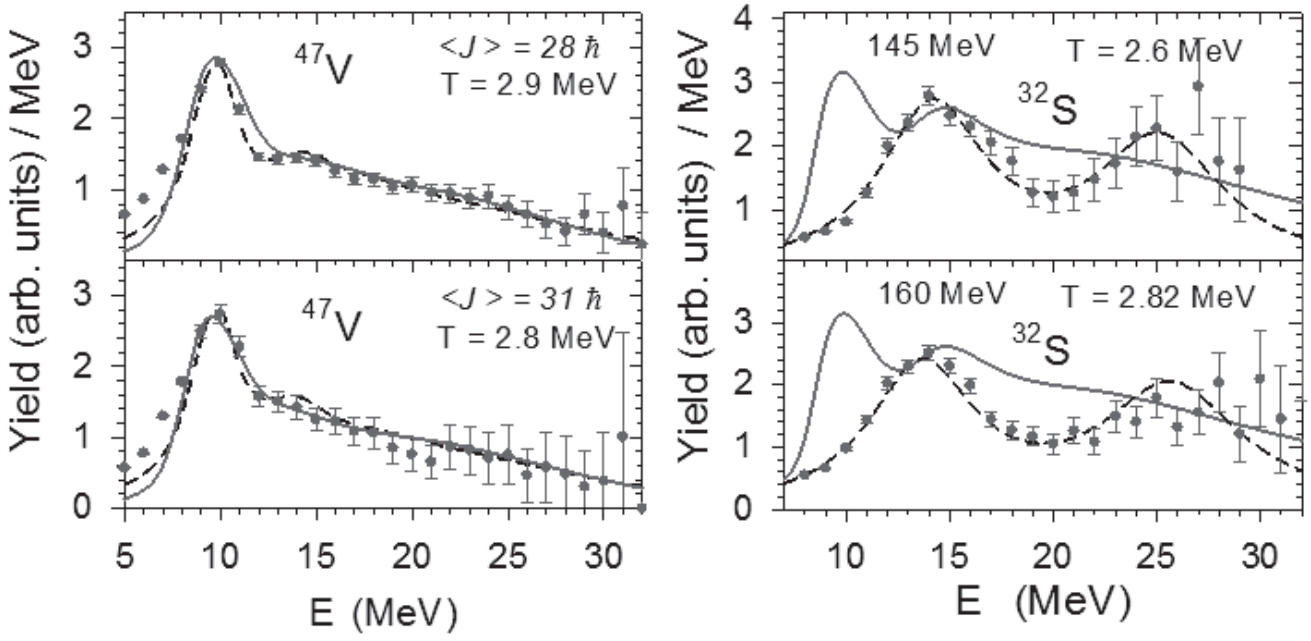

Figure 3: Linearized GDR lineshapes for ^{47}V and ^{32}S. The symbols, dashed lines and continuous lines represent the experimental data, GDR strength functions used in CASCADE and TSFM predictions, respectively.

case of a spherical or a near spherical system [1, 14] and indicate large deformations. The most striking feature for ^{47}V is the strong enhancement in the γ-ray yield at $\sim$ 10 MeV. It is the characteristics of Jacobi shape transition and the effect of Coriolis splitting due to very high angular velocity in the system [5, 8, 15]. However, for ^{32}S no such enhancement is seen even though the nucleus is populated at spins well beyond Jacobi transition point. A two-component GDR strength function fits the experimental data fairly well. The shape looks more like a highly extended prolate (one component at $\sim$ 14 MeV and another at $\sim$ 26 MeV) and is seen for the first time for this nucleus [5, 8].

In order to understand the equilibrium deformation in these hot and rotating nuclear systems, a calculation was performed for estimating the equilibrium shape of a nucleus by minimizing the total free energy under the framework of rotating liquid drop model (RLDM) and thermal shape fluctuation model (TSFM) for a given temperature and angular momentum [16, 17, 18]. The free energy for a hot rotating liquid drop at constant spin and neglecting the shell effects is given as [8, 18]

$$F = E_{LDM} - TS + \frac{J(J+1)\hbar}{2(\vec{\omega}\cdot I\cdot\vec{\omega})} \qquad (2)$$

where E_{LDM} is the deformed liquid drop energy, S is the entropy and $\vec{\omega}\cdot I\cdot\vec{\omega}$ is the moment of inertia about the rotation axis ω. The dependence of level densities on deformation and shell corrections are assumed to be small and neglected as the nuclear temperatures in this case are around 3 MeV. The deformed liquid drop energy (E_{LDM}) was calculated for different shapes [19, 20, 21, 22] along with the deformation dependent moment of inertia according to Hill-Wheeler parameterization (β, γ) [17, 18]. The free energy surfaces for ^{47}V are shown in Figure 4 at different spins. The equilibrium deformation was obtained from the minimization of the free energy surfaces at different spins and is plotted in Figure 5 for ^{47}V and ^{32}S. It is clearly seen, at low spins the nucleus is oblate ($\gamma = 60^{\circ}$) and its de-

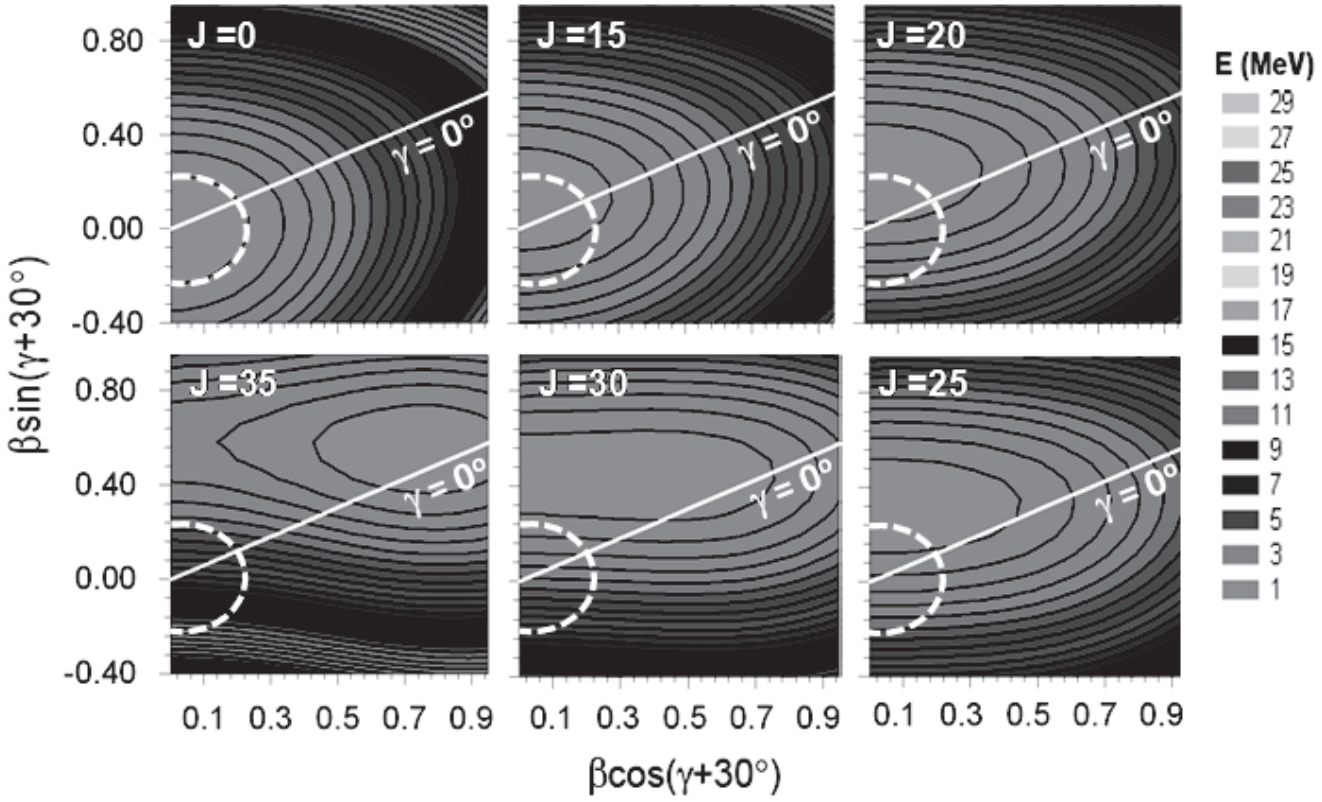

Figure 4: Liquid drop free energy surfaces at different spins of ^{47}V. The line represents the prolate shape ($\gamma = 0°$) while the dotted line corresponds to minimum of the free energy at $J = 0\hbar$. The free energy surfaces are shown with increasing angular momentum in clockwise direction staring from top left corner.

formation increases with spin. However, above a certain critical spin ($J = 28\hbar$ and $J = 18\hbar$ for ^{47}V and ^{32}S, respectively) nucleus becomes triaxial and finally becomes nearly collective prolate ($\gamma = 0°$) characterized by large deformations ($\beta \sim 0.7$).

In general, for a non-rotating nucleus, the GDR strength functions along the 3 axes for an ellipsoidal shape can be obtained using the Hill-Wheeler parameterization $E_k = E_0 \exp[-\sqrt{(}5/4\pi)\beta\cos(\gamma - 2\pi k/3)]$ with $k = 1, 2, 3$ denoting the three principal axes. E_0 refers to the centroid energy for a spherical nucleus with mass A. However, these frequencies are modified in the case of a rotating nucleus. A rotating anisotropic harmonic oscillator potential and the isovector dipole-dipole interaction term describe the empirical energy of the giant dipole resonance [23]. In this approach, the two GDR components split (which are perpendicular to the rotation axis) due to Coriolis effect as the GDR vibrations in a nucleus couple with its rotation. The third component (along the rotation axis) remains intact. This gives altogether five components in general for the GDR strength function. However, all five of these frequencies do not exist for all the shapes of the nuclei. They exist only for a collectively rotating triaxial nucleus as well as for a prolate nucleus rotating about an axis perpendicular to its symmetry axis. For non collective oblate nuclei only two components will exist. Therefore, the total GDR cross section can be written, in general, as

$$\sigma = \sum_{i=1}^{n} \frac{\Gamma_i^2 E_\gamma^2}{(E_\gamma^2 - E_i^2)^2 + \Gamma_i^2 E_\gamma^2} \qquad (3)$$

where E_i and Γ_i are the centroid energies and GDR

widths, respectively, of the resonance. Here i represents the number of components of the GDR and is determined from the shape of the nucleus. The energy dependence of the GDR width is approximated by $\Gamma_i = 0.029E_i^{1.9}$. The free energy minimization technique gives the most likely deformations for the nucleus under consideration at particular temperature and angular momentum. However, at high temperatures the nuclear shape fluctuates around the equilibrium deformation which will influence the response of nuclei for dipole radiation. In a first approximation, it can be assumed that the changes in the shape parameters are slow compared to the GDR vibrations. Therefore, the resultant GDR lineshape is obtained as a superposition of all the components (E_i, Γ_i) averaged over the entire deformation space due to thermal fluctuations using

$$\langle\sigma\rangle = \frac{\int D_\alpha e^{-F}/T(\vec{\omega}\cdot I\cdot\vec{\omega})^{-3/2}\sigma}{\int D_\alpha e^{-F}/T(\vec{\omega}\cdot I\cdot\vec{\omega})^{-3/2}} \qquad (4)$$

where $D_\alpha = \beta^4\cdot|\sin(3\gamma)|d\beta\, d\gamma$ is the volume element [8, 16].

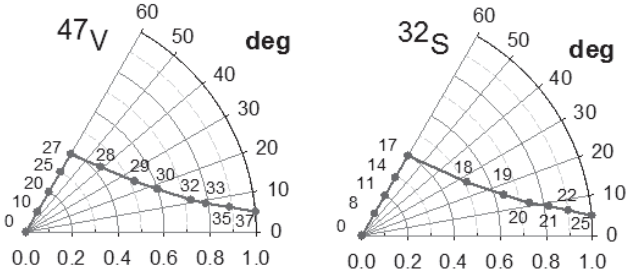

Figure 5: The equilibrium shapes are plotted as a function of quadrupole deformation parameters (β, γ) and for different spins for ^{47}V and ^{32}S.

The theoretical lineshapes are compared with the experimental data in Figure 3. As can be seen, it describes the data for ^{47}V remarkably well for both the experimentally measured spin windows of $28\hbar$ and $31\hbar$ at corresponding temperatures of 2.9 and 2.8 MeV, respectively. This remarkable good agreement between the theoretical predictions and the present experimental results is very much in favour of the onset of the Jacobi shape transition [5, 8, 15, 24]. Moreover, the appearance of a GDR component at ~ 10 MeV is only possible due to the Coriolis splitting at very high angular frequency of the lowest vibrational frequency (which corresponds to the dipole vibration along the longest axis of the well deformed prolate or triaxial shape). In fact, for oblate shapes, typical for the equilibrium deformation at rotational frequencies lower than the critical value for the Jacobi transition, the Coriolis splitting is always absent [23]. On the other hand, the same free energy calculation fails miserably to explain the GDR strength function for ^{32}S performed at both low and high angular momenta.

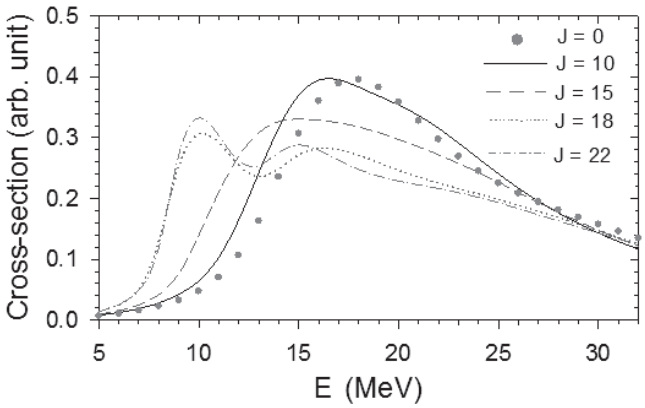

Figure 6: The evolution of GDR lineshape with angular momentum for ^{32}S nucleus at $T = 2.8$ MeV.

The evolution of the GDR lineshape as function of J for ^{32}S at $T = 2.8$ MeV is shown in Figure 6. The calculation performed at $J = 22\hbar$ & $T = 2.8$ MeV is shown in Figure 3. The deformation [1] was calculated from the two GDR peaks obtained experimentally and was found to be $\beta = 0.76$ which corresponds to an axis ratio of $\sim 2:1$ at 160 MeV incident energy. The occurrence of such a large deformation without showing the characteristics of Jacobi transition could be due to the formation of a

Table 1: The extracted GDR components for two angular momentum windows for ^{47}V.

$\langle J \rangle = 28\hbar$			$\langle J \rangle = 28\hbar$		
E_i (MeV)	Γ_i (MeV)	S_i	E_i (MeV)	Γ_i (MeV)	S_i
9.9 ± 0.5	3.0 ± 0.5	0.18 ± 0.02	9.9 ± 0.4	3.0 ± 0.5	0.18 ± 0.03
14.5 ± 0.4	5.3 ± 1.1	0.16 ± 0.04	14.1 ± 0.6	5.1 ± 0.9	0.16 ± 0.06
18.3 ± 1.0	8.1 ± 0.9	0.19 ± 0.06	18.4 ± 0.8	8.4 ± 1.1	0.19 ± 0.08
23.1 ± 0.8	11.3 ± 1.4	0.20 ± 0.08	23.0 ± 1.2	11.5 ± 1.7	0.20 ± 0.08
27.3 ± 1.5	15.5 ± 1.7	0.27 ± 0.10	27.8 ± 1.8	15.8 ± 2.0	0.27 ± 0.11

Table 2: The extracted GDR parameters for ^{32}S at two beam energies.

$E_{\mathrm{lab}} = 145$ MeV			$E_{\mathrm{lab}} = 160$ MeV		
E_i (MeV)	Γ_i (MeV)	S_i	E_i (MeV)	Γ_i (MeV)	S_i
14.5 ± 0.3	6.2 ± 0.8	0.37 ± 0.05	14.0 ± 0.4	6.2 ± 0.9	0.32 ± 0.05
25.4 ± 0.8	7.5 ± 1.3	0.63 ± 0.09	26.0 ± 0.9	8.2 ± 1.8	0.68 ± 0.10

long lived, highly deformed orbiting dinuclear complex where the nucleus is not fully equilibrated (in terms of shape degrees of freedom) and maintains the entrance channel shape before finally splitting into two parts [4]. In our charge particle experiment for ^{20}Ne ($\sim$ 7–10 MeV/nucleon) + ^{12}C reactions, yields of carbon and boron fragments were significantly enhanced, which indicated the survival of orbiting at these high excitation energies [25, 26]. However, it can also be conjectured that the observed unusual deformation can be due to the formation of the molecular structure of the $^{16}\mathrm{O} + {}^{16}\mathrm{O}$ cluster in ^{32}S. In the theoretical work of Kimura and Horiuchi, it was predicted that the superdeformed states of ^{32}S have considerable amount of $^{16}\mathrm{O} + {}^{16}\mathrm{O}$ components and become more prominent as the excitation energy increases [27]. The estimated deformation for two touching ^{16}O was found to be $\beta = 0.73$ which is in agreement with the experimentally extracted deformation from the resonance energy peaks ($\beta = 0.76$).

Thus, the result presented in this work clearly shows that the GDR γ-decay can be effectively used to study different reaction mechanisms and the importance of the selecting high rotational frequencies in the investigation of nuclear shapes.

Acknowledgments

I am grateful and wish to thank Dr. S. R. Banerjee, Dr. Alokkumar De, Dr. Surajit Pal, Dr. Supriya Mukhopadhyay and Dr. Srijit Bhattacharya for their constant support and encouragement to complete this work.

References

[1] J. J. Gaardhoje, *Annu. Rev. Nucl. Part. Sci.* **42**, 483 (1992).

[2] S. Chandrasekhar, "Ellipsoidal figures of equilibrium", Yale Univ. Press, New Haven, (1969).

[3] C. Beck *et al., Phys. Rev.* **C80**, 034604 (references therein) (2009).

[4] S. J. Sanders *et al., Phys. Rep.* **311**, 487 (1999).

[5] Deepak Pandit, PhD Thesis, (2013), Homi Bhabha National Institute.

[6] S. Mukhopadhayay *et al., Nucl. Inst. Methods* **A582**, 603 (2007).

[7] Deepak. Pandit *et al., Nucl. Inst. Methods* **A624**, 148 (2010).

[8] Deepak. Pandit *et al., Phys. Rev.* **C81**, 061302 (Rapid) (2010).

[9] Dimitri Kusnezov *et al., Phys. Rev. Lett.* **90**, 042501 (2003).

[10] Puhlhofer, *Nucl. Phys.* **A280**, 267 (1977).

[11] Srijit Bhattacharya *et al., Phys. Rev.* **C77**, 024318 (2008).

[12] H. Nifennecker *et al., Annu. Rev. Nucl. Part. Sci.* **40** 113 (1990).

[13] A. V. Ignatyuk *et al., Sov. J. Nucl. Phys.* **21**, 255 (1975).

[14] Deepak. Pandit *et al., Phys. Lett.* **B713**, 434 (2012).

[15] A. Maj *et al., Nucl. Phys.* **A731**, 319 (2004).

[16] Y. Alhassid *et al., Phys. Rev. Lett.* **65**, 2527 (1990).

[17] P. Arumugam *et al., Phys. Rev.* **C69**, 054313 (2004).

[18] Y. Alhassid *et al., Nucl. Phys.* **A565**, 427 (1993).

[19] W. D. Myers *et al., Nucl. Phys.* **81**, 1 (1966).

[20] P. Moller *et al., Nucl. Phys.* **A361**, 117 (1981).

[21] K. T. R. Davies *et al., Phys. Rev.* **C14**, 1977 (1976).

[22] H. J. Krappe *et al., Phys. Rev.* **C20**, 992 (1979).

[23] K. Neergard, *Phys. Lett.* **B110**, 7 (1982).

[24] D. R. Chakrabarty *et al., Phys. Rev.* **C85**, 044619 (2012).

[25] Aparajita Dey *et al., Phys. Rev.* **C74**, 044605 (2006).

[26] C. Bhattacharya *et al., Phys. Rev.* **C72**, 021601 (Rapid) (2005).

[27] Masaaki Kimura et al., Phys. Rev. **C69**, 051304 (Rapid) (2004).

Dr. Deepak Pandit did his M.Sc. from IIT, Kharagpur and joined BARC Training School. Later he joined VECC and obtained his Ph.D. Degree in Physics from Homi Bhabha National Institute in 2013. He played a major role in developing the Large Area Modular BaF2 Detector Array. He has made significant contributions both in experimental nuclear structure physics and nuclear theory. He has published many papers in international journals. Dr. Pandit has been conferred the Young Scientist Award for the year 2013 and the Group Achievement Award for the year 2009 in the DAE Award Scheme for his outstanding research contributions in the field of Experimental Nuclear Physics. He received the Second best YPC award in 2014.